Available online at www.sciencedirect.com
SCIENCE DIRECT®
J. of Supercritical Fluids 33 (2005) 209–222
THE JOURNAL OF Supercritical Fluids
www.elsevier.com/locate/supflu

Isochoric heat capacity measurements for a CO_2 + *n*-decane mixture in the near-critical and supercritical regions☆

Nikolai G. Polikhronidi[a], Rabiyat G. Batyrova[a], Ilmutdin M. Abdulagatov[a,b,*], Joseph W. Magee[b], Genadii V. Stepanov[a]

[a] *Institute of Physics of the Dagestan Scientific Center of the Russian Academy of Sciences, Makhachkala, Russia*
[b] *Physical and Chemical Properties Division, National Institute of Standards and Technology, 325 Broadway, Boulder, CO 80305, USA*

Received 27 January 2004; accepted 30 August 2004

Abstract

The isochoric heat capacity of a (0.7367 mole fraction) CO_2 + (0.2633 mole fraction) *n*-decane mixture was measured in a range of temperatures from 362 to 577 K, at nine near-critical liquid and vapor densities between 298 and 521 kg m^{-3} by using a high-temperature, high-pressure, nearly constant volume adiabatic calorimeter. The measurements were performed in both one- and two-phase regions including the vapor + liquid coexistence curve. Uncertainties of the heat capacity measurements are estimated to be 2% (in this work we use a coverage factor $k = 2$). The uncertainty in temperature is 10 mK and that for density measurements is 0.15%. The liquid and vapor one- (C'_{V1}, C''_{V1}) and two-phase (C'_{V2}, C''_{V2}) isochoric heat capacities, temperatures (T_S) and densities (ρ_S) at saturation were extracted from the experimental data for each filling density. The critical temperature ($T_C = 509.71 \pm 0.2$ K), the critical density ($\rho_C = 344.7 \pm 5$ kg m^{-3}), and the critical pressure ($P_C = 15.37 \pm 0.5$ MPa) for the (0.7367 mole fraction) CO_2 + (0.2633 mole fraction) *n*-decane mixture were extracted from isochoric heat capacity measurements using the well-established method of quasi-static thermograms. The observed isochoric heat capacity along the critical isochore of the CO_2 + *n*-decane mixture exhibits a renormalization of the critical behavior of C_V unlike that of the pure components. The ranges of conditions were defined, on the *T*–*x* plane for the critical isochore and the ρ–*x* plane for the critical isotherm, for which we observed renormalization of the critical behavior for isochoric heat capacity. The Krichevskii parameter for this mixture was calculated by using the critical loci for the mixture and vapor pressure data for the pure solvent (CO_2), and the results are compared with published values.

Keywords: Adiabatic calorimeter; Carbon dioxide; Coexistence curve; Critical point; Equation of state; Krichevskii parameter; Isochoric heat capacity; *n*-Decane; Supercritical fluid mixture

1. Introduction

Industry continues to widely exploit the anomalous properties of supercritical fluids [1–3]. Supercritical fluids are of fundamental importance in geology and mineralogy (for hydrothermal synthesis), in chemistry, in the oil and gas industries, and for some new separation techniques, especially in supercritical fluid extraction. Supercritical fluids have also been proposed as a solvent or reaction medium for a number of technological applications including coal conversion, organic synthesis, destructive oxidation of hazardous wastes (SCWO processes), enhanced oil recovery, activated carbon regeneration, formation of inorganic films and powders, supercritical chromatography, organic reaction rate modification and precipitation polymerization [1–3]. Supercritical carbon dioxide is widely used as a solvent in supercritical fluid extractions and supercritical fluid chromatography [4–7]. A supercritical carbon dioxide solvent has been proposed for a number of separation and reaction processes [7,8].

The thermodynamic properties of CO_2 + *n*-decane mixtures are of interest to the petroleum and natural gas industry, primarily because of the growing interest in the extraction

☆ Contribution of the National Institute of Standards and Technology, not subject to copyright in the United State.

* Corresponding author. Tel.: +1 303 497 4027; fax: +1 303 497 5224.
E-mail address: ilmutdin@boulder.nist.gov (I.M. Abdulagatov).

0896-8446/$ – see front matter © 2004 Elsevier B.V. All rights reserved.
doi:10.1016/j.supflu.2004.08.009

of viscous, low volatility compounds with supercritical CO_2 in tertiary oil recovery and new separation techniques. Near-critical and supercritical carbon dioxide has been used as a miscible flooding agent that promotes miscible displacement of hydrocarbons from underground reservoirs [9]. To improve our understanding of the mechanism of the process of miscible displacement of reservoir oils by carbon dioxide injection (oil recovery enhancement) and control those processes, a better knowledge of model systems would be helpful. Since *n*-decane is a typical component of petroleum, and is available as a high-purity ambient-temperature liquid, it makes a good choice for a model system. Precise measurements are needed to establish the behavior of the thermodynamic properties of CO_2 + *n*-decane mixtures. Although our understanding of the thermodynamic properties of CO_2 and binary (CO_2 + solute) systems at ambient conditions has improved significantly, it is far from sufficient to accurately predict the behavior of (CO_2 + solute) systems for the near-critical and supercritical conditions that are currently of great scientific and practical interest. Therefore, to use supercritical CO_2 effectively, it will be necessary to know the thermodynamic properties of CO_2 + solute mixtures at supercritical conditions.

In addition, an important theoretical question is centered upon near-critical and supercritical phenomena in systems for which one of the components is near its critical point [10–12]. For example, there is great theoretical interest in negatively or positively diverging solute partial molar properties ($\bar{V}_2^{\infty}$, $\bar{H}_2^{\infty}$, $\bar{C}_{P2}^{\infty}$) in the immediate vicinity of the solvent's critical point and path-dependence of the solvent properties in near-critical systems [10–12]. The critical region behavior of CO_2 + *n*-decane mixtures is also of theoretical interest, for example, to determine how *n*-decane molecules affect the critical region behavior of carbon dioxide or to examine consequences of the isomorphism principle on the critical region behavior of CO_2 + *n*-decane mixtures. The shape of the critical locus curve is of great importance for studying the real critical behavior of mixtures, since the shape of the critical locus is very sensitive to differences in molecular size and interactions of the components. Binary mixtures of CO_2 with *n*-alkanes belong to three different types in the well-known classification by van Konynenburg and Scott [13]. In this scheme, the systems CO_2 + (C_2 to C_4) are type I, CO_2 + *n*-C_8 is type II, and CO_2 + *n*-C_{16} is type III. This illustrates the possible complexity that can be observed experimentally for binary mixtures of this class.

Published measurements of the thermodynamic properties of CO_2 + *n*-decane are scarce. Furthermore, reports of caloric properties, in particular the isochoric heat capacity of CO_2 + *n*-decane mixtures, are unknown. Thus, the main objective of this work is to provide new reliable experimental isochoric heat capacity data for CO_2 + *n*-decane mixtures in the critical and supercritical regions. Due to a scarcity of experimental (*PVTx* and $C_V VTx$) data, it is not yet possible to understand the effect of the solvent's critical region properties on the thermodynamic behavior of a CO_2 + *n*-decane mixture or to develop an accurate scaling type equation of state. Thus, in this work we report $C_V VTx$ properties of a mixture of (0.7367 mole fraction) CO_2 + (0.2633 mole fraction) *n*-decane measured using a high-temperature, high-pressure, nearly constant-volume adiabatic calorimeter in the temperature range between 362 and 577 K and the density range from 298 to 521 kg m^{-3}. Previously, we reported the isochoric heat capacity of the pure components CO_2 [14,15] and *n*-decane [16] in the near-critical and supercritical regions. The same apparatus was used to measure C_V for the CO_2 + *n*-decane mixture. Prior to this work, thermodynamic properties of CO_2 + *n*-decane mixtures have been reported [17–23]. Table 1 shows the available thermodynamic data sets for CO_2 + *n*-decane mixtures. In this table, the first author and the year published are given together with the method employed, the uncertainty indicated by the authors, and the temperature, pressure, and concentration ranges. As expected, experimental isochoric heat capacity data for CO_2 + *n*-decane mixtures were not available in the literature. Most of the available *PVTx* and *VLE* data cover only limited ranges of temperature, pressure, and concentration. Thus, the primary objective of this work was to expand the existing thermodynamic database for the CO_2 + *n*-decane mixtures. The available experimental critical curve data sets are given in Table 2. A brief synopsis of the different data sets is given below.

Nagarajan and Robinson [18] reported experimental vapor–liquid equilibrium phase compositions and phase densities (ρ'_S, ρ''_S) for the CO_2 + *n*-decane mixtures at two temperatures of 344.3 and 377.6 K and at pressures to the critical point. The phase compositions are in excellent agreement with the data reported by Reamer and Sage [17], however, the phase densities exhibit significant differences. In this case, the values of the critical density reported by Nagarajan and Robinson [18] are substantially higher than values reported by Reamer and Sage [17].

Recently Shaver et al. [21] reported liquid and vapor equilibrium phase compositions, phase densities, and interface tensions for the CO_2 + *n*-decane mixtures at 344.3 K. By using an extrapolation technique, they derived the values of the critical parameters (T_C, P_C, and ρ_C) for the composition $x = 0.065$ mol fraction of CO_2. The phase densities measured by Shaver et al. [21] and those of Nagarajan and Robinson [18] show excellent agreement. However, fairly large disagreement exists between these two data sets and the data of Reamer and Sage [17]. The liquid densities reported by Shaver et al. [21] are lower than those of Reamer and Sage [17] with the largest differences near the critical point. The liquid compositions reported by Shaver et al. [21] agree with all of the published data sets within 0.005 mole fraction CO_2 except those of Chou et al. [22]. The vapor phase compositions reported by Shaver et al. [21] are in good agreement with those of Nagarajan and Robinson [18] at low pressures, but differences near the critical point are about 0.006 mole fraction CO_2. The critical pressure reported by Shaver et al. [21] (P_C = 12.714 MPa) is in good agreement with the value (P_C = 12.741 MPa) derived by Nagarajan and Robinson [18]

Table 1
Summary of the thermodynamic property measurements for CO_2 + *n*-decane mixtures

First author	Year	Method	Property	Uncertainty	Temperature (K)	Pressure (MPa)	Concentration (mole fraction)
Reamer [17]	1963	VVP	*VLE* (*PTx*) *PVTx*	0.01% (*P*), 0.05 K, 0.0039 m.f., 0.15–0.30% (*V*)	278–510	up to 19	0–1
Nagarajan [18]	1986	VTD	*VLE* (*PTx*) (ρ'_S, ρ''_S)	0.5 kg m^{-3}, 0.014 MPa	344.3 and 377.6	up to P_C	0.13–0.93
Polikhronidi [20]	1997	HTHPAC	*PVTx*	0.02 MPa, 0.01 K, 0.05% (ρ)	290–570	up to 25	0.178
Shaver [21]	2001	HPEC	*VLE* (*PTx*) (ρ'_S, ρ''_S)	±1.0 kg m^{-3}, ±0.014 MPa, ±0.06 K, ±0.003 m.f.	344.3	up to 35	0.108–0.935
Chou [22]	1990	SEA	*VLE* (*PTx*)	0.2 K, 0.2–0.5 MPa, 0.002–0.005 m.f.	290.25 and 377.55	4.1–15.5	0.315–0.999
Bufkin [23]	1986	–	Solubility	–	–	1.3–8.6	–

HPEC, high pressure equilibrium cell; HTHPAC, high temperature, high pressure adiabatic calorimeter; SEA, static equilibrium apparatus; VVP, variable volume piezometer; VTD, vibration U-tube densimeter; n.a., no uncertainty given in source reference.

but disagrees with the value (P_C = 12.824 MPa) reported by Reamer and Sage [17].

2. Experimental

The apparatus used for the C_{VX} measurements of CO_2 + *n*-decane mixtures has been described previously [24–30] and was used without modification. Since the construction of the calorimeter and the experimental procedures has been described in detail in several previous publications [24–30], they will only be briefly reviewed here. The isochoric heat capacities were measured with a high-temperature, high-pressure, adiabatic, and nearly constant-volume calorimeter, which offers an expanded uncertainty (k = 2) of 2% of the heat capacity. The volume of the calorimeter, 105.126 ± 0.13 cm^3 at atmospheric pressure and 297.15 K, is well-known as a function of temperature and pressure. The calorimeter volume was determined by using measured *PVT* data for a standard fluid (pure water) with well-known *PVT* values calculated with the IAPWS formulation [31]. Our uncertainty in the determination of volume at any T and P is about 0.13%. The mass of the sample was measured by using a weighing method with an uncertainty of 0.05 mg (or 0.005%). Therefore, the maximum uncertainty in the measurements of density $\rho = m/V$ (P, T) is about 0.15%. The heat capacity was obtained from measurements of the following quantities: m, mass of the fluid; ΔQ, electrical energy released by the inner heater; ΔT, temperature rise resulting from addition of an energy ΔQ; and C_0 is the empty calorimeter heat capacity. The thermometer was calibrated on the ITS-90 scale. The uncertainty of temperature measurements is 10 mK. A detailed uncertainty analysis of the method (all of the measured quantities and corrections) is given in several previous papers [24–30]. In earlier work, Polikhronidi et al. [29] reported the heat capacity of the empty calorimeter C_0, determined by using a reference substance (helium-4) with well-known isobaric heat capacities (Vargaftik [32]), over a temperature range up to 1000 K at pressures up to 20 MPa. The uncertainty in the C_P data used for calibration of C_0 is 0.2% [32]. A small energy correction related to the stretching of the cell during heating was determined with an uncertainty of about 4.0–9.5% of the correction, depending on the density. The absolute uncertainty in C_V due to departures from full adiabatic control is 0.013 kJ K^{-1}. The combined standard uncertainty related to the indirect character of the C_V measurements did not exceed 0.16%. Based on a detailed analysis of all sources of uncertainties likely to affect the determination of C_V with the present system, the combined expanded (k = 2) uncertainty of measured heat capacity is 2%.

Table 2
Summary of the critical property measurements for CO_2 + *n*-decane mixtures

First author	Property	Uncertainty in T_C measurements (K)	Uncertainty in P_C measurements (MPa)	Uncertainty in ρ_C measurements (kg m^{-3})	Concentration range (mole fraction)
Reamer [17]	T_C, ρ_C, P_C	n.a.	n.a.	n.a.	0–1
Nagarajan [18]	T_C, ρ_C, P_C	n.a.	n.a.	n.a.	0.930, 0.895
Gulari [19]	T_C, ρ_C, P_C	±(0.02–0.03)	n.a.	n.a.	0.004–0.028
Polikhronidi [20]	T_C, ρ_C, P_C	±0.2	±0.5	±5	0.178
Shaver [21]	T_C, ρ_C, P_C	n.a.	n.a.	n.a.	0.935
Gurdial [50]	T_C, P_C	±0.2	±0.05	–	0.003–0.023

Heat capacity was measured as a function of temperature at nearly constant density. The calorimeter was filled at room temperature, sealed off, and heated along a quasi-isochore. Each run for the heat capacity was normally started in the two-phase region and completed in the one-phase region at its highest temperature or pressure. This method enables one to determine, with a good accuracy, the transition temperature T_S of the system from the two-phase to a single-phase state (i.e., to determine T_S and ρ_S data corresponding to the phase-coexistence curve), the jump in the heat capacity ΔC_V, as well as reliable C_V data in the single- and two-phase regions [28,33,34]. The technique used to determine the T_S and ρ_S at the coexistence curve and of measuring the heat capacity C_V at this curve is the method of quasi-static thermograms as described in detail in our previous papers [28,33,34]. The method of quasi-static thermograms makes it possible to obtain reliable phase transition temperatures, including a critical temperature, with an uncertainty of 0.01–0.02 K.

To check the method and confirm the reliability of phase transitions and critical point parameters by means of the quasi-static thermogram technique, phase transition temperature measurements were made on pure distilled water in our previous study [30] with the same apparatus. We reported measured values of a phase transition temperature $T_S = 647.104 \pm 0.003$ K (run-1) and $T_S = 647.109 \pm 0.003$ (run-2) for a near-critical filling density of 321.96 kg m^{-3}, which are both in very close agreement with the critical temperature $T_C = 647.096$ K adopted by the IAPWS-95 standard formulation [31]. An agreement for the two measurements of 8 and 13 mK is within our estimated uncertainty and helps to confirm the reliability of the quasi-static thermogram technique to determine phase transition temperatures for pure fluids and mixtures.

3. Results and discussion

Measurements of the isochoric heat capacity for a CO_2 + *n*-decane mixture ($x = 0.2633$ mole fraction of *n*-decane) were carried out on nine filling densities: (liquid) 358.9, 372.8, 409.8, 466.9, and 520.6 kg m^{-3}; (vapor) 298.7, 312.6, 328.9 kg m^{-3}; and (critical) 344.7 kg m^{-3}. The experimental temperature range was 362–577 K. In total, 156 C_{VX} measurements are reported for the one- and two-phase regions in Table 3. On the coexistence curve, a total of 18 values of C_{VX} and T_S were measured close to the critical point (see Table 4). The experimental one-phase liquid (C'_{V1}) and vapor (C''_{V1}), two-phase liquid (C'_{V2}) and vapor (C''_{V2}) data, and the values of temperature (T_S) and density (ρ_S) at saturation are also presented in Table 4.

Figs. 1 and 2 depict the temperature dependence of the measured values of isochoric heat capacities for the CO_2 + *n*-decane mixture. As shown in these figures, for each isochore, the heat capacity C_{VX} rises with temperature increasing to a maximum at the phase transition temperature T_S,

Table 3
Experimental values of the one-phase and two-phase isochoric heat capacities of the CO_2 + *n*-decane mixture at near-critical densities

T (K)	C_{VX} (kJ kg^{-1} K^{-1})
$\rho = 520.6$ kg m^{-3}	
372.127	9.26
385.456	9.25
398.965	9.30
402.407	9.43
416.643	9.51
429.771	9.74
443.068	10.04
444.080	9.97
446.100	9.97
448.317	10.12
452.532[a]	**10.22**[a]
452.532[a]	**8.74**[a]
453.931	8.57
456.921	8.53
468.370	8.41
485.616	8.57
$\rho = 466.9$ kg m^{-3}	
371.678	9.21
395.503	9.17
419.373	9.62
443.270	9.97
461.876	10.70
471.107	10.54
473.447	11.04
475.099	**11.00**
475.099	**9.13**
476.942	9.08
477.523	8.90
479.381	8.99
479.651	8.89
479.072	9.01
495.902	8.69
514.066	8.96
$\rho = 409.8$ kg m^{-3}	
362.638	9.35
475.361	11.15
485.424	11.71
486.670	11.79
487.818	11.86
489.249	12.03
490.203	12.04
490.584	12.08
490.870	**12.11**
490.870	**9.96**
491.155	9.91
492.107	9.91
493.057	9.84
494.386	9.77
496.848	9.69
$\rho = 372.8$ kg m^{-3}	
476.264	11.28
481.772	11.51
487.530	11.73
493.437	12.05
499.304	12.68
500.057	12.70
500.434	12.82
500.904	12.88
501.187	**12.96**

Table 3 (*Continued*)

T (K)	C_{VX} (kJ kg^{-1} K^{-1})
501.187	**10.66**
501.563	10.51
501.939	10.44
502.127	10.42
502.315	10.48
507.000	10.19
510.451	10.10
520.725	10.15
ρ = 358.9 kg m^{-3}	
475.779	11.29
484.081	11.65
495.144	12.13
503.066	12.80
503.816	12.97
504.379	13.08
504.942	13.20
505.316	**13.36**
505.316	**11.01**
505.460	10.89
506.054	10.78
506.252	10.58
509.426	10.37
510.078	10.25
513.889	10.25
525.868	10.10
537.340	9.97
ρ = 344.7 kg m^{-3}	
485.807	11.72
495.144	12.18
504.379	12.79
506.252	13.00
507.747	13.21
508.951	13.34
509.352	13.52
509.560	13.78
509.705	**13.87**
509.705	**11.43**
509.799	11.34
509.892	11.29
509.985	11.23
510.171	11.15
510.357	10.98
510.710	10.95
511.960	10.76
519.805	10.33
530.529	10.21
542.400	10.15
554.056	10.15
ρ = 328.9 kg m^{-3}	
507.000	16.74
507.560	13.06
508.120	13.06
513.147	13.54
513.332	13.62
513.704	13.71
514.260	13.91
514.445	**13.95**
514.445	**11.25**
515.001	10.99
515.371	10.96
515.927	10.94
516.297	10.89
522.014	10.45

Table 3 (*Continued*)

T (K)	C_{VX} (kJ kg^{-1} K^{-1})
522.565	10.48
531.529	10.42
539.873	10.30
550.661	10.23
560.819	10.30
567.900	10.18
ρ = 312.6 kg m^{-3}	
494.955	12.37
504.567	12.79
505.129	12.85
513.518	13.44
515.002	13.54
515.186	13.57
516.944	13.83
517.591	13.93
518.145	14.05
518.698	14.27
519.344	**14.34**
519.344	**11.21**
521.186	10.73
520.910	11.12
531.711	10.73
541.498	10.46
550.302	10.48
559.932	10.48
568.608	10.56
576.966	10.50
ρ = 298.7 kg m^{-3}	
494.575	12.50
505.877	13.02
513.704	13.42
522.197	14.13
522.749	14.30
524.034	14.48
524.584	14.58
525.685	**14.99**
525.685	**11.17**
526.051	11.12
526.600	10.98
546.358	10.79
556.264	10.83
566.663	10.83

x = 0.2633 mole fraction of *n*-decane.

[a] One- and two-phase saturation points.

Table 4

Experimental values of the isochoric heat capacities (C'_{V1}, C''_{V1}), temperatures (T_S), and densities (ρ_S) of the CO_2 + *n*-decane mixture on the saturation boundary

T_S (K)	ρ'_S (kg m^{-3})	C'_{V1} (kJ kg^{-1} K^{-1})	C'_{V2} (kJ kg^{-1} K^{-1})
452.53	520.6	8.74	10.22
475.10	466.9	9.13	11.00
490.87	409.8	9.96	12.11
501.19	372.8	10.66	12.96
505.32	358.9	11.01	13.36
509.71 (cr.)	344.7 (cr.)	11.43	13.87
T_S (K)	ρ''_S (kg m^{-3})	C''_{V1} (kJ kg^{-1} K^{-1})	C''_{V2} (kJ kg^{-1} K^{-1})
514.45	328.9	11.25	13.95
519.34	312.6	11.21	14.34
525.69	298.7	11.17	14.99

x = 0.2633 mole fraction of *n*-decane.

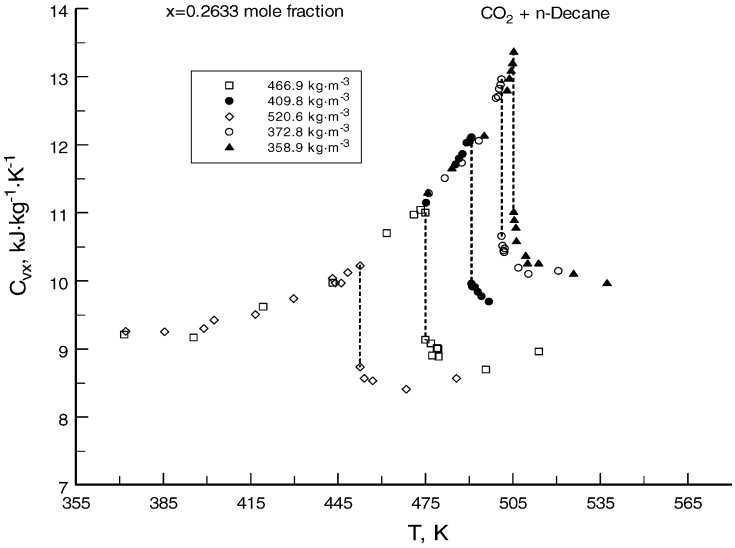

Fig. 1. Experimental one- and two-phase isochoric heat capacities of the CO_2 + *n*-decane as a function of temperature on near-critical liquid isochores. Dashed lines are isochoric heat capacity jumps at the phase transition temperatures for each density.

and then drops discontinuously to a value corresponding to that of the one-phase region. By changing the amount of sample in the calorimeter, it is possible to obtain a complete set of C_{V1} and C_{V2} at saturation temperatures. As Figs. 1 and 2 show, along each isochore, C_{VX} exhibits a jump at the transition from a two-phase state (left of phase transition temperature T_S) to a homogeneous one-phase state (right of phase transition temperature T_S). Each jump measurement (see Figs. 1 and 2) is one point on the two dimensional T_S–ρ_S phase boundary plane and supplies values for one-C_{V1} and two-phase C_{V2} heat capacities at this condition (at saturation temperature T_S). Thus, the C_{VX} experiment provides useful information about saturated properties (T_S, ρ_S, C_{V1}, and C_{V2}) near the critical point and, as a result, the values of the critical properties (T_C, ρ_C) of the mixture. The isochoric heat capacities of pure components (CO_2 and *n*-decane) near the critical point were previously reported by Abdulagatov et al. [14,15] and Amirkhanov et al. [16]. The specific volume dependence of the two-phase isochoric heat capacities of the CO_2 + *n*-decane mixture along various near-critical isotherms is shown in Fig. 3 together with values of C_{VX} on the coexistence curve. In contrast to the linear behavior observed for every pure fluid, the two-phase isothermal C_{VX}–V dependence for the binary mixture CO_2 + *n*-decane was observed to be a non-linear function of V.

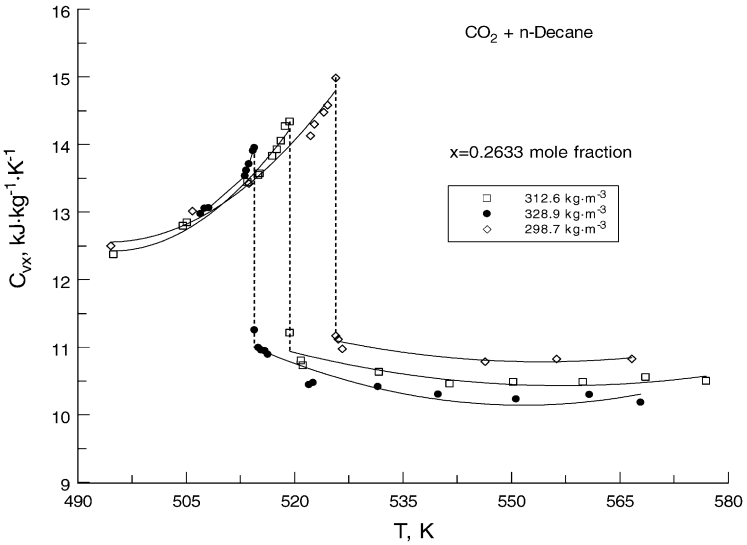

Fig. 2. Experimental one- and two-phase isochoric heat capacities of the CO_2 + *n*-decane as a function of temperature on near-critical vapor isochores. The solid lines are guides for the eye. Dashed lines are isochoric heat capacity jumps at the phase transition temperatures for each density.

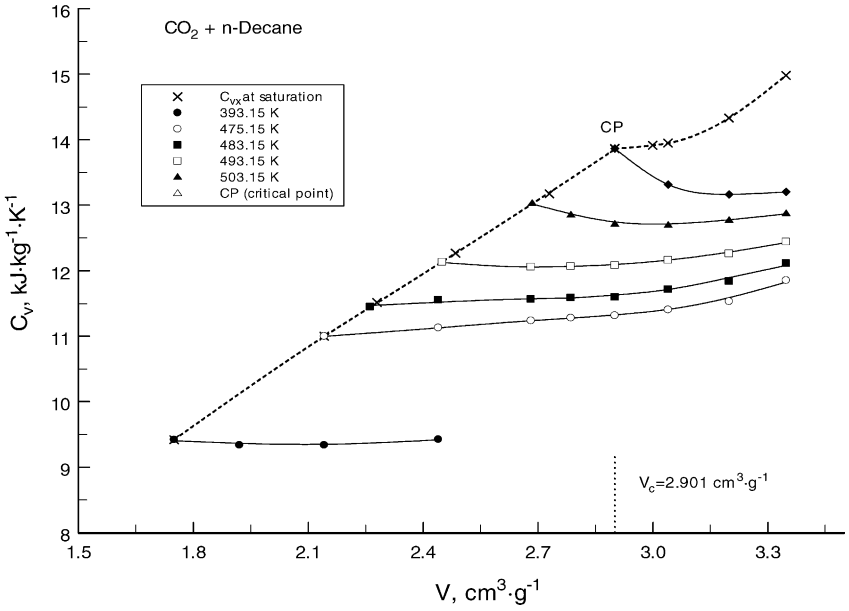

Fig. 3. Experimental two-phase isochoric heat capacities of the CO_2 + *n*-decane as a function of specific volume on near-critical isotherms. The solid lines are guides for the eye. Dashed line is the saturation curve.

Fig. 4 illustrates the temperature dependence of the liquid and vapor one- and two-phase isochoric heat capacity of the CO_2 + *n*-decane mixture at saturation near the critical point. As shown in Fig. 4, which depicts the temperature dependence of the one-phase (C_{V1}–T curve) and two-phase (C_{V2}–T curve) at saturation, a break point (liquid–vapor critical point) was observed for the mixture. It is shown that while C_{V1} and C_{V2} monotonically increases with temperature up to the critical point, an abrupt change of the slope is observed at the break point. At the transition from the liquid densities to those of the vapor, both the C_{V1}–T and C_{V2}–T curves have a change of slope (break point). At this break point, the liquid and vapor become identical, providing the temperature, density, and concentrations of the critical parameters of the mixture. From our experimental C_{VX} and (T_S–ρ_S) measurements on the coexistence curve for CO_2 + *n*-decane mixtures, we have deduced the values for the critical temperature T_C and the critical density ρ_C. Our results are $T_C = 509.71 \pm 0.2$ K, $P_C = 15.37 \pm 0.5$ MPa, and $\rho_C = 344.7 \pm 5$ kg m^{-3}, which are in fair agreement with those data $T_C = 510.01$ K, $P_C = 15.66$ MPa, and $\rho_C = 353.1$ kg m^{-3} reported by Reamer and Sage [17] (see Figs. 5–7) at nearly the same composition.

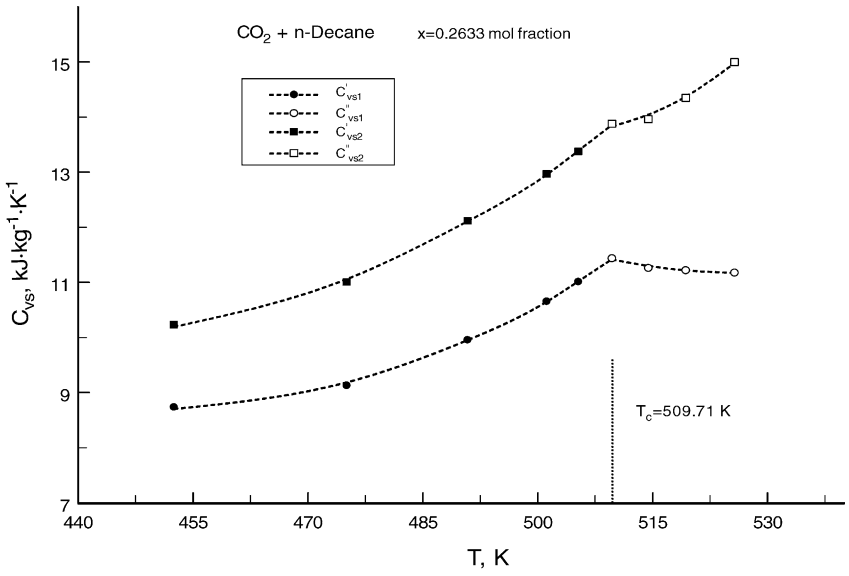

Fig. 4. Experimental values of liquid and vapor one-phase (C'_{V1}, C''_{V1}) and two-phase (C'_{V2}, C''_{V2}) isochoric heat capacities on the coexistence curve as a function of temperature near the critical point. The dashed lines are guides for the eye.

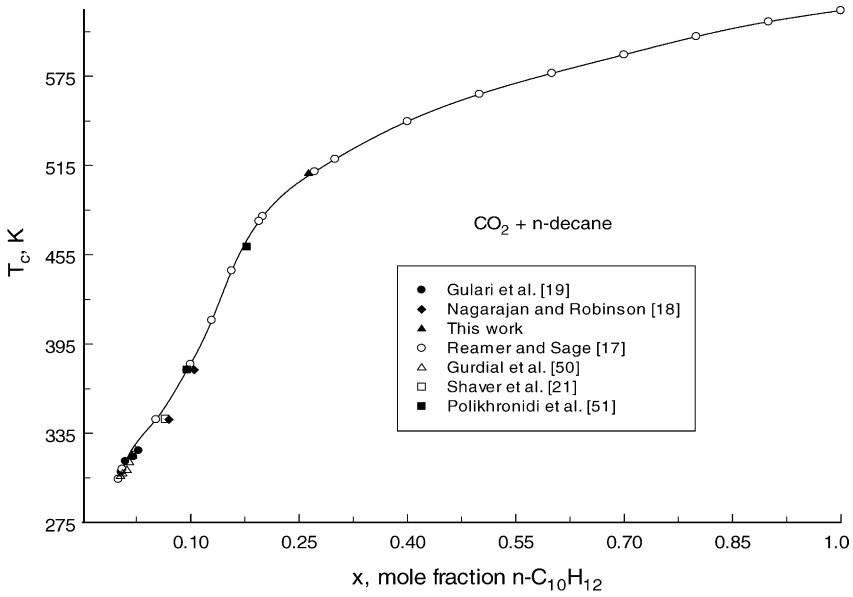

Fig. 5. The critical temperatures of CO_2 + *n*-decane mixtures as a function of concentration. The solid lines are guides for the eye.

Figs. 5–7 show the present critical data and the curves (T_C–x, P_C–x, and ρ_C–x) data for CO_2 + *n*-decane mixtures reported previously by various authors. The T_C–P_C critical locus for CO_2 + *n*-decane mixtures together with vapor pressure curves for the pure components are depicted in Fig. 8. As one can see, the consistency between this work and published measurements of the critical parameters is good, except a few data points reported by Reamer and Sage [17] for the critical densities at low concentrations of *n*-decane. For a composition of 0.2633 mole fraction of *n*-decane, the difference between the present critical temperature and the data reported by Reamer and Sage [17] is 0.3 K, an amount that is very close to their uncertainty. Satisfactory agreement within 2.4% was found between the critical density reported by Reamer and Sage [17] and the present result for 0.2633 mole fraction. Satisfactory agreement of 1.9% was found between the critical pressure reported by Reamer and Sage [17] and the present result.

In this work, closely spaced measurements were made in the critical region and near every phase transition point, providing essential information for an accurate determination of both the critical parameters and for saturated temperatures and densities near the critical point. Figs. 9 and 10 show the measured vapor–liquid coexistence curve (T_S–ρ_S) for the CO_2 + *n*-decane mixture which were determined from C_{VX} experiments by using the method of quasi-static thermograms

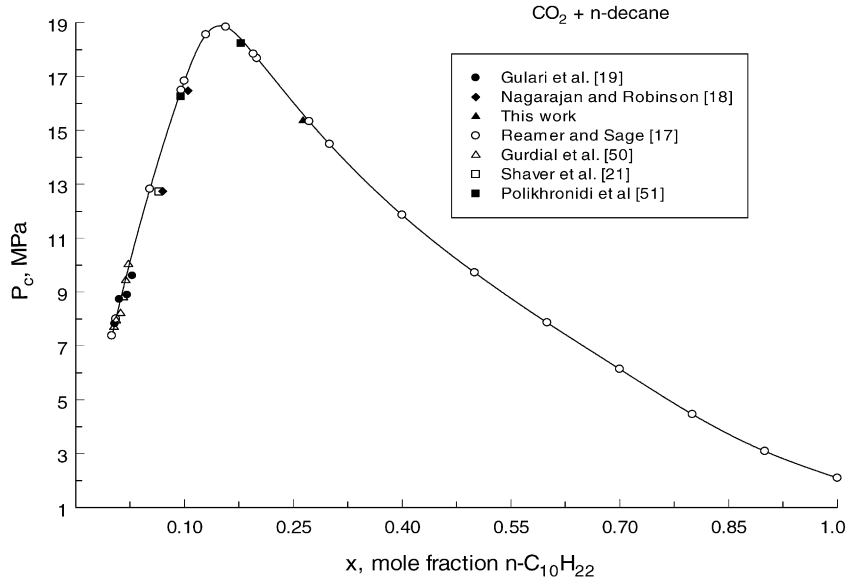

Fig. 6. The critical pressures of CO_2 + *n*-decane mixtures as a function of concentration. The dashed lines are guides for the eye [51].

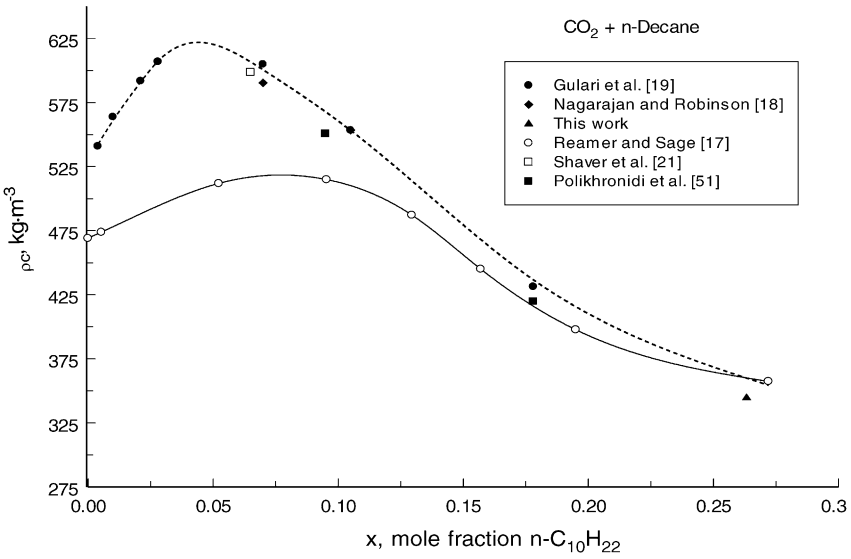

Fig. 7. The critical densities of CO_2 + *n*-decane mixtures as a function of concentration. The dashed lines are guides for the eye.

[28,33] along with the vapor–liquid coexistence curves of both pure components near the critical point calculated with the Lemmon and Span [35] (*n*-decane) and Span and Wagner [36] and (CO_2) multiparameter equations of state. As one can see from Fig. 10, the shape of the liquid–vapor coexistence curve near the critical point for mixture is a dramatic change from the flat top of the dome seen for pure fluids. Additional information given in Figs. 9 and 10 are the loci of critical points. A very small, but noticeable, anomaly of the liquid–vapor coexistence curve can be seen near the critical point in the T_S–ρ_S plane (see Fig. 9) that would be difficult to detect by means of *PVTx* experiments alone. The shape of the liquid–vapor coexistence curve near the critical point has two inflection points, which bracket the critical point [37]. The critical point for this mixture does not coincide with the maximum temperature point, $(\partial T_S/\partial \rho_S)_x \neq 0$, of the liquid–vapor coexistence curve. This is why few investigations report this anomalous behavior, which has been discussed from a theoretical perspective by Rainwater [37].

As Figs. 9 and 10 show, the agreement between the present and published data is satisfactory, with deviations within 0.07–0.17%.

Comprehensive studies of the consequences of the isomorphism principle on the critical behavior of mixtures have been presented by Anisimov and coworkers [38–41]. According to the isomorphism principle, near-critical behavior of binary fluids is controlled by two characteristic parameters K_1 and K_2, which are determined by the slope of the critical locus.

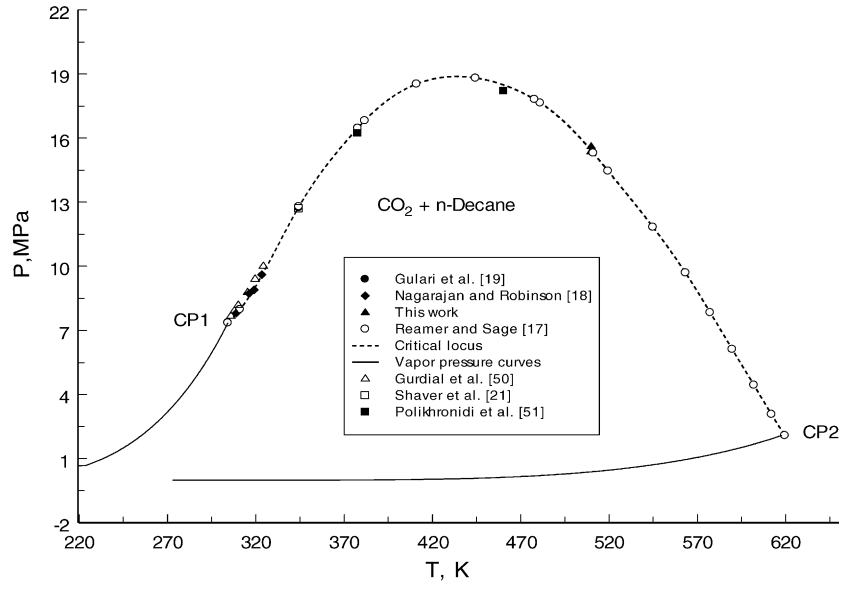

Fig. 8. The critical locus of CO_2 + *n*-decane mixture together with vapor pressure curves for the pure components. The dashed lines are guides for the eye.

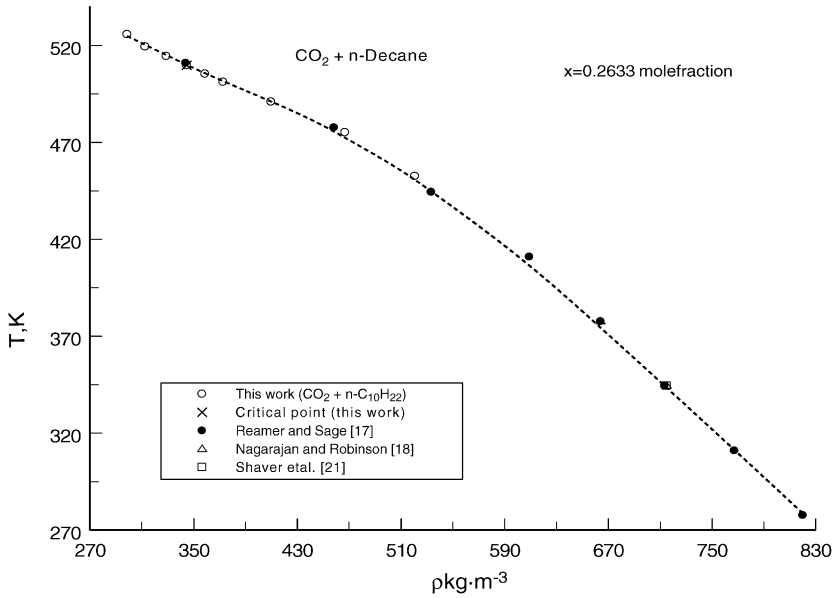

Fig. 9. The experimental liquid and vapor densities at saturation for CO_2 + *n*-decane from C_{VX} experiments (quasi-static thermogram technique).

The parameter K_1 is responsible for strongly divergent properties such as the isothermal compressibility K_T and isobaric heat capacity C_P, while the parameter K_2 controls the weakly divergent properties like the isochoric heat capacity C_V and defines the range of Fisher renormalization of the critical exponents [42]. The parameters K_1 and K_2 are defined [43] by:

$$K_1 = \frac{x(1-x)}{\rho_C R T_C}\left[\frac{dP_C}{dx} - \left(\frac{\partial P}{\partial T}\right)^c_{\xi,\rho=\rho_C}\frac{dT_C}{dx}\right] \quad (1)$$

and

$$K_2 = \frac{x(1-x)}{T_C}\frac{dT_C}{dx}. \quad (2)$$

Correspondingly, two characteristic temperature differences τ_1 and τ_2 and two characteristic density differences $\Delta\bar{\rho}_1$ and $\Delta\bar{\rho}_2$ are defined through K_1 and K_2

$$\tau_1 = \left[\frac{\Gamma_0^+ K_1^2}{x(1-x)}\right]^{1/\gamma}, \quad (3)$$

$$\tau_2 = \left[\frac{A_0^+ K_2^2}{x(1-x)}\right]^{1/\alpha}, \quad (4)$$

$$\Delta\bar{\rho}_1 = B_0 \tau_1^\beta, \quad (5)$$

and

$$\Delta\bar{\rho}_2 = B_0 \tau_2^\beta, \quad (6)$$

where $\tau = (T_C - T)/T_C$ and $\Delta\rho = (\rho_C - \rho)/\rho_C$. For CO_2, the asymptotic critical amplitudes [44] are $A_0^+ = 26.36$, $B_0 = 1.708$, and $\Gamma_0^+ = 0.056$ of the power laws for isochoric heat capacity, the coexistence curve, and the isothermal compressibility, respectively, and the universal critical exponents for C_V are $\alpha = 0.112$ and for the coexistence curve $\beta = 0.325$ [45]. In the dilute solution limit ($x \to 0$), the expression between the brackets in Eq. (1) for K_1 reduces to the Krichevskii parameter K_{kr} [43,46,47]

$$K_{kr} = \lim_{X\to 0}\left(\frac{\partial P}{\partial x}\right)^C_{V_C T_C},$$

$$\left(\frac{\partial P}{\partial x}\right)^C_{V_C T_C} = \left(\frac{\partial P_c}{\partial x}\right)^C_{CRL} - \left(\frac{dP_S}{dT}\right)^C_{CXC}\left(\frac{\partial T_c}{\partial x}\right)^C_{CRL} \quad (7)$$

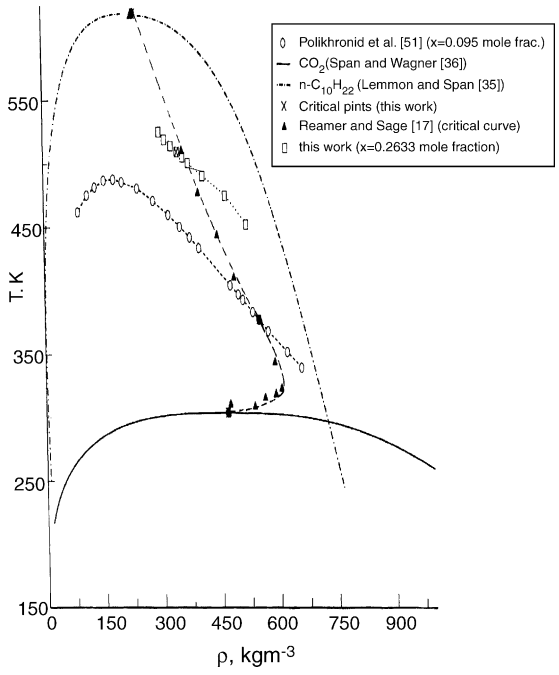

Fig. 10. The coexistence curves for CO_2 + *n*-decane mixtures and their pure components. The dashed lines are guides for the eye.

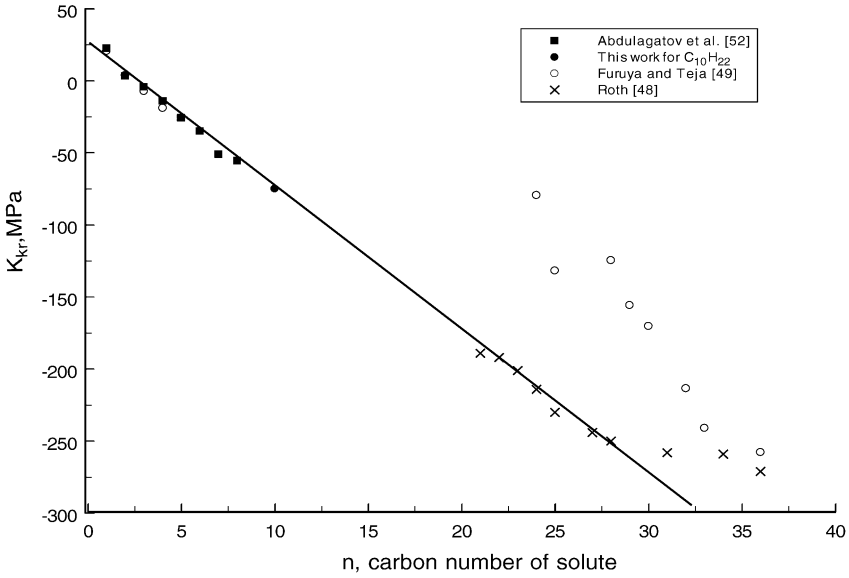

Fig. 11. The Krichevskii parameters of CO_2 + *n*-alkane mixtures as a function of solute carbon number. The solid line is guides for the eye [52].

or, equivalently

$$\left(\frac{\partial P}{\partial x}\right)^{C}_{V_C T_C} = \left[\left(\frac{\mathrm{d}P_c}{\mathrm{d}T_c}\right)^{C}_{\mathrm{CRL}} - \left(\frac{\mathrm{d}P_S}{\mathrm{d}T}\right)^{C}_{\mathrm{CXC}}\right]\left(\frac{\mathrm{d}T_c}{\mathrm{d}x}\right)^{C}_{\mathrm{CRL}}, \tag{8}$$

where values of the initial critical locus slopes for the CO_2 + *n*-decane mixture at infinite dilution ($x \to 0$) were determined from the present and published (Reamer and Sage [17], Nagarajan and Robinson [18] and Gulari et al. [19]) critical curve data to be $\mathrm{d}T_C/\mathrm{d}x|_{X\to 0} = 1274.53 \pm 10$ K, $\mathrm{d}P_C/\mathrm{d}x|_{X\to 0} = 126.2 \pm 3$ MPa, and $(\partial P_C/\partial T_C)^{C}_{\mathrm{CRL}} = 0.1126\ \mathrm{MPa\,K^{-1}}$. In order to calculate the values of $\mathrm{d}T_C/\mathrm{d}x|_{X\to 0}$ and $\mathrm{d}P_C/\mathrm{d}x|_{X\to 0}$ the present and published experimental critical curve data for CO_2 + *n*-decane mixture were fitted to a polynomial type of function for the critical temperatures and critical pressures as a function of composition

$$T_C(x) = T_C(CO_2) + \left(\frac{\mathrm{d}T_C}{\mathrm{d}x}\right)_{x=0} x + T_1 x^2 + \cdots, \tag{9}$$

$$P_C(x) = P_C(CO_2) + \left(\frac{\mathrm{d}P_C}{\mathrm{d}x}\right)_{x=0} x + P_1 x^2 + \cdots, \tag{10}$$

where $T_C(CO_2) = 304.136$ K and $P_C(CO_2) = 7.3773$ MPa are the critical temperature and the critical pressure of pure carbon dioxide. The quantity $(\mathrm{d}P_S/\mathrm{d}T)^{C}_{\mathrm{CXC}} = 0.1712\ \mathrm{MPa\,K^{-1}}$, which is the slope of the vapor pressure curve of the solvent (carbon dioxide), was calculated with the vapor pressure correlation of Span and Wagner [36]. Substitution of these values of the derivatives into Eq. (7) resulted in a Krichevski parameter $K_{kr} = -74.75 \pm 5$ MPa. Fig. 11 shows reported Krichevskii parameters for CO_2 + *n*-alkane mixtures as a function of solute carbon number, together with our value for the CO_2 + *n*-decane mixture derived in this work. As this figure shows, the present result for the CO_2 + *n*-decane mixture is consistent with the data reported by Roth [48] for other CO_2 + *n*-alkane mixtures, while the data reported by Furuya and Teja [49] are systematically higher.

According isomorphism principle [38–42], along the critical isochore in the one-phase region, all properties of a binary fluid mixture will exhibit the same behavior as those of a pure fluid in a range of temperatures $\tau \gg \tau_1$ and $\tau \gg \tau_2$. At $\tau_2 < \tau < \tau_1$, properties that exhibit strong singularities in one-component fluids (associated with the critical exponent γ) will reach a plateau, however, weakly singular properties (associated with the critical exponent α) will continue to grow. At $\tau < \tau_2$, those properties that diverge weakly in one-component fluids will be saturated and all critical exponents will be renormalized by the factor $1/(1-\alpha)$. In terms of density, along the critical isotherm the behavior of all properties will be one-component-like at densities $|\Delta\overline{\rho}| \gg \pm\Delta\overline{\rho}_1$ ("−" for the $\rho > \rho_C$ and "+" for the $\rho > \rho_C$) and the Fisher renormalization occurs at $|\Delta\overline{\rho}| \ll \pm\Delta\overline{\rho}_2$ [41]. At $\tau \ll \tau_2$, the isochoric heat capacity behavior of a binary mixture will be renormalized by a factor $1/(1-\alpha)$ (Fisher renormalization [42]). In terms of density, along the critical isotherm the behavior of isochoric heat capacity will be renormalized at densities $|\Delta\rho| \ll \Delta\rho_2$. The values of K_1, τ_1, K_2, τ_2, $\Delta\rho_1$, and $\Delta\rho_2$ calculated from Eqs. (1) to (6) for a CO_2 + *n*-decane mixture at $x = 0.2633$ are: −2.985, 2.1, 1.133, 2.4×10^{17}, 2.35, and 1.49×10^6, respectively. The concentration dependence of $T_C(x)$ is steep enough, $\mathrm{d}T_C/\mathrm{d}x|_{X\to 0} = 996.9 \pm 10$ K, therefore, the renormalization of the critical exponents can be detected for this mixture. Fig. 12 shows concentration dependence of the characteristic temperatures (τ_1, τ_2) and characteristic density differences ($\Delta\overline{\rho}_1$, $\Delta\overline{\rho}_2$) for the CO_2 + *n*-decane mixture ($x = 0.2633$ mole fraction of *n*-decane). As one can see from this figure, the characteristic temperatures and densities (τ_2, $\Delta\overline{\rho}_2$) change very sharply with an increas-

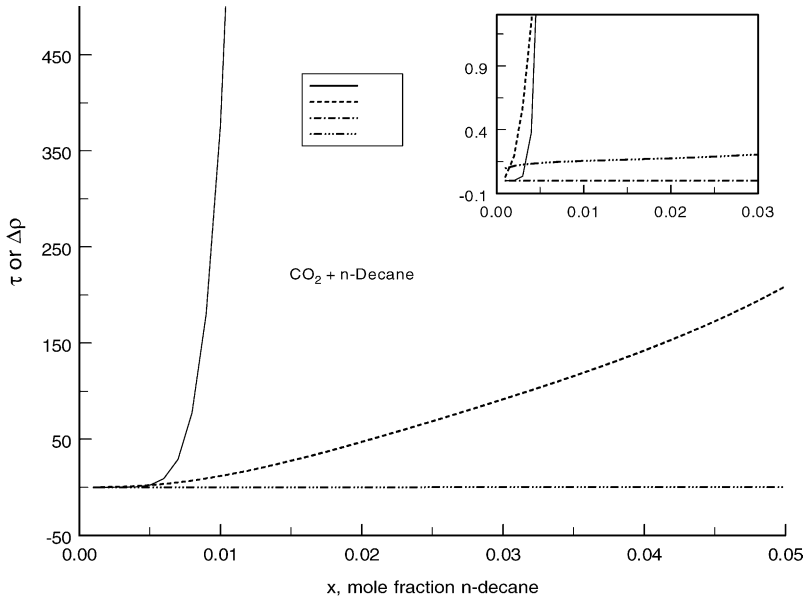

Fig. 12. Characteristic temperatures (τ_1 and τ_2) and densities ($\Delta\rho_1$ and $\Delta\rho_2$) as a function of the concentration of *n*-decane. (—) τ_2; (- - - - - -) $\Delta\rho_2$; (-·-·-·-·-·-) τ_1; and (-···-···-···-) $\Delta\rho_1$.

ing concentration of *n*-decane, while the values of (τ_1 and $\Delta\overline{\rho}_1$) change only very weakly. Values of τ_2 and $\Delta\rho_2$ are very high for this composition. Therefore, measured in this work temperatures τ significantly lower than τ_2 ($\tau \ll \tau_2$, experimentally accessible temperature range). This is means that C_{VX} behavior which diverge weakly for pure CO_2 ($x = 0$) with exponent $\alpha = 0.12$, $C_V \propto \tau^{-\alpha}$, will be renormalized by the factor $1/(1-\alpha)$, $C_{VX} \propto \tau^{\alpha/(1-\alpha)}$. The isochoric heat capacity measurements for CO_2 + *n*-decane mixture ($x = 0.2633$ mole fraction) reported in this work, along the critical isochore, confirm Fisher renormalization of the critical exponent for C_{VX} (see Fig. 13). Fig. 13 shows experimental $\log C_{VX}$ for the CO_2 + *n*-decane mixture and for the pure components along their respective critical isochores as a function of $\log \tau$. As this figure shows, the slopes of the $\log C_{VX} - \log \tau$ curves for the mixtures are almost zero, while for the pure components the slopes are both very close to the scaling value of 0.112. This means that, when approaching the critical point ($\tau \to 0$) along the critical isochore, the singular or fluctuation part of the heat capacity C_{VX} for the CO_2 + *n*-decane mixture is zero ($C_{VX} \sim \tau^{\alpha/(1-\alpha)}$). Therefore, isochoric heat capacity of the CO_2 + *n*-decane mixture ($x = 0.2633$ mole fraction) at the critical point behaves without any singularity. The behavior of the isochoric heat capacity C_{VX} at the critical point

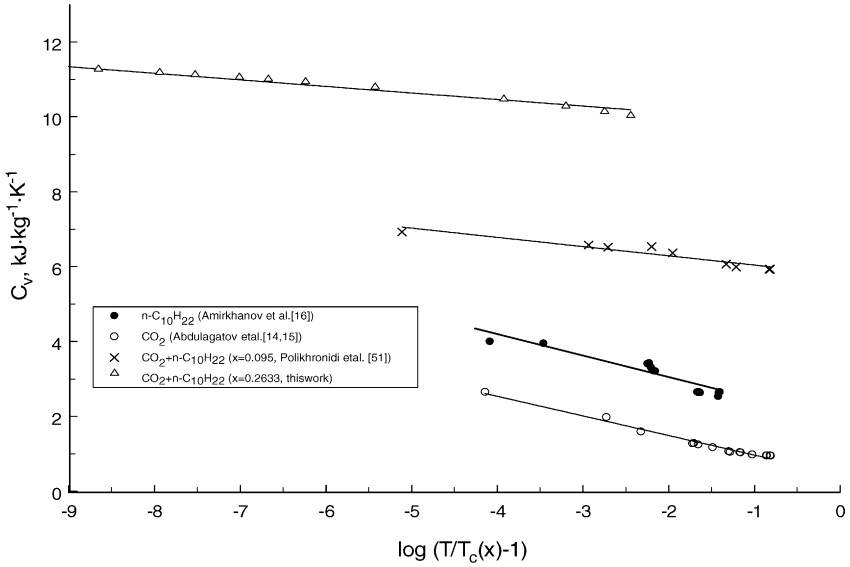

Fig. 13. Isochoric heat capacities ($\log C_{VX}$) of the CO_2 + *n*-decane mixture and their pure components as a function of $\log \tau$ on their critical isochores in the asymptotic regions. The solid lines are guides for the eye.

would be completely determined by the regular part (background term); therefore, C_{VX} for this mixture is constant, at the critical point, because C_{VX} exhibits a finite cusp with an infinite slope. The fluctuation-induced, analytic, background contribution to C_{VX} vanishes at the critical point of a mixture. When composition of the mixture approaches the values of the pure components ($x \to 0$ or $x \to 1$) the trends of C_{VX} would sharply change to pure fluid behavior, while for any other composition C_{VX} data exhibit mixture-like behavior (renormalization of the critical exponent).

4. Conclusion

Isochoric heat capacities were measured for the (0.7367 mole fraction) CO_2 + (0.2633 mole fraction) *n*-decane mixture in a temperature range from 362 to 577 K, at nine near-critical densities, namely: 298.7, 312.6, 328.9, 344.7 (critical density), 358.9, 372.8, 409.8, 466.9, and 520.6 kg m^{-3} by using a high-temperature, high-pressure, nearly constant volume adiabatic calorimeter. The reported measurements include both the one-phase and two-phase regions, and the coexistence curve near the critical point. Uncertainties of the C_{VX} and phase transition temperature measurements are estimated to be within 2% and 0.02 K, respectively. The values of temperatures and densities at saturation (T_S, ρ_S) and the critical parameters (T_C, ρ_C, P_C) were extracted from C_{VX} measurement using the quasi-static thermogram technique. The derived values of the critical parameters together with values reported by other authors were used to calculate the values of the Krichevskii parameter for the CO_2 + *n*-decane mixture. The measured values of the critical parameters are in good agreement with the values reported in the literature by other authors. The measured results are used to analyze the critical behavior of isochoric heat capacity of the CO_2 + *n*-decane mixture in terms of the principle of isomorphism of critical phenomena. The analysis showed that experimental isochoric heat capacity data for the CO_2 + *n*-decane mixture with a composition of 0.2633 mole fraction of *n*-decane confirms Fisher renormalization by a factor $1/(1-\alpha)$, unlike that observed for the pure components. The ranges were defined in the *T*–*x* for the critical isochore and the ρ–*x* planes for the critical isotherm where renormalization of the critical behavior of isochoric heat capacity occurs. The values of the characteristic temperatures (τ_1, τ_2) and the characteristic density differences ($\Delta\bar{\rho}_1$, $\Delta\bar{\rho}_2$) were estimated using the critical curve data and modern theory of critical phenomena in binary mixtures.

Acknowledgment

One of us (I.M.A.) thanks the Physical and Chemical Properties Division at the National Institute of Standards and Technology for the opportunity to work as a Guest Researcher at NIST during the course of this research.

References

[1] E. Kiran, J.M.H. Levelt Sengers (Eds.), Supercritical Fluids Fundamentals for Application, vol. 273, ASI Ser., NATO, 1993.
[2] E. Kiran, J.F. Brennecke (Eds.), Supercritical Fluid Engineering Science, Symp. Ser. 514, ACS, Washington, DC, 1993.
[3] E.U. Franck, Supercritical water, steam, water, and hydrothermal systems: physical and chemistry meeting the needs of industry, in: P.R. Tremaine, P.G. Hill, D.E. Irish, P.V. Balakrishnam (Eds.), Proceedings of the 13th International Conference on Prop. Water and Steam, NRC Research Press, 2000, pp. 22–34.
[4] G.M. Schneider, Applications of fluid mixtures and supercritical solvents: a survey, in: E. Kiran, J.M.H. Levelt Sengers (Eds.), Supercritical Fluids, Kluwer, Dordrecht, 1994, pp. 739–757.
[5] M. McHugh, V. Krukonis, Supercritical Fluid Extraction, Butterworths, London, 1986.
[6] G.M. Schneider, E. Stahl, G. Wilke (Eds.), Extraction with Supercritical Gases, Verlag Chemie, Weinheim, 1980, p. 189.
[7] G.M. Schneider, in: M. Perrut (Ed.), Proceedings of the International Symposium on Supercritical Fluids, Nice, France, 1988, pp. 1–17.
[8] S. Saito, Research activities on supercritical fluid science and technology in Japan—a review, J. Supercrit. Fluids 8 (1995) 177–204.
[9] T.M. Doscher, M. El-Arabi, Scale model experiments show how CO_2 might economically recover residual oil, Oil Gas J. 80 (1982) 144–158.
[10] J.M.H. Levelt Sengers, Thermodynamics of solutions near the solvent's critical point, in: J.F. Ely, T.J. Bruno (Eds.), Supercritical Fluid Technology, CRC Press, Boca Raton, FL, 1991, p. 1.
[11] R.F. Chang, J.M.H. Levelt Sengers, Behavior of dilute mixtures near the solvent's critical point, J. Phys. Chem. 90 (1986) 5921–5927.
[12] J.M.H. Levelt Sengers, Solubility near the solvent's critical point, J. Supercrit. Fluids 4 (1991) 215–222.
[13] P.H. van Konynenburg, R.L. Scott, Critical lines and phase equilibria in binary van der Waals mixtures, Phils. Trans. R. Soc. London A 298 (1980) 495–540.
[14] I.M. Abdulagatov, N.G. Polikhronidi, R.G. Batyrova, Measurements of the heat capacities C_V of carbon dioxide in the critical region, J. Chem. Thermodyn. 26 (1994) 1031–1045.
[15] I.M. Abdulagatov, N.G. Polikhronidi, R.G. Batyrova, Isochoric heat capacity and liquid–gas coexistence curve of carbon dioxide in the region of the immediate vicinity of the critical point, Ber. Bunsenges Phys. Chem. (1994) 98.
[16] Kh.I. Amirkhanov, D.I. Vikhrov, B.G. Alibekov, V.A. Mirskaya, Isochoric Heat Capacities and Other Caloric Properties of Hydrocarbons, Dagestan Scientific Center of the Russian Academy of Sciences, Makhachkala, 1981.
[17] H.H. Reamer, B.H. Sage, Phase equilibria in hydrocarbon systems. Volumetric and phase behavior of the *n*-decane–CO_2 system, J. Chem. Eng. Data 8 (1963) 508–513.
[18] N. Nagarajan, R.L. Robinson, Equilibrium phase compositions, phase densities, and interfacial tensions for CO_2 + hydrocarbon systems. 2. CO_2 + *n*-decane, J. Chem. Eng. Data 31 (1986) 168–171.
[19] E.S. Gulari, H. Saad, V.C. Bae, Effect of critical phenomena on transport properties in the supercritical region, in: T.G. Squires, M.E. Paulaitis (Eds.), Supercritical Fluids. Chemical and Engineering Principles and Applications, ACS Symp. Ser. 329, Washington, DC, 1987, pp. 2–14.
[20] N.G. Polikhronidi, R.G. Batyrova, *PVT* measurements for the binary CO_2 + n-decane system, Russ. High Temp. 35 (1997) 537–541.
[21] R.D. Shaver, R.L. Robinson, K.A.M. Gasem, An automated apparatus for equilibrium phase compositions, densities, and interfacial tensions: data for carbon dioxide, Fluid Phase Equilib. 179 (2001) 43–66.
[22] G.F. Chou, R.R. Forbert, J.M. Prausnitz, High-pressure vapor–liquid equilibria for CO_2/decane, CO_2/tetralin, and CO_2/decane/tetralin at 71.1 and 104.4 °C, J. Chem. Eng. Data 35 (1990) 26–29.

[23] B. Bufkin, High pressure solubilities of carbon dioxide and ethane in selected paraffinic, naphthenic and aromatic solvents, M.S. Thesis, Oklahoma State University, Stillwater, OK, 1986.
[24] N.G. Polikhronidi, R.G. Batyrova, I.M. Abdulagatov, Isochoric heat capacity measurements of nitrogen tetroxide system at temperatures between 410 and 484 K and pressures up to 35 MPa, Fluid Phase Equilib. 175 (2000) 153–174.
[25] N.G. Polikhronidi, R.G. Batyrova, I.M. Abdulagatov, Two-phase heat capacity measurements for nitrogen tetroxide in the critical region and Yang–Yang relation, Int. J. Thermophys. 21 (2000) 1073–1096.
[26] N.G. Polikhronidi, I.M. Abdulagatov, J.W. Magee, R.G. Batyrova, Isochoric heat capacity for toluene near phase transitions and the critical point, J. Chem. Eng. Data 46 (2001) 1064–1071.
[27] N.G. Polikhronidi, I.M. Abdulagatov, J.W. Magee, G.V. Stepanov, Isochoric heat capacity measurements for light and heavy water near the critical point, Int. J. Thermophys. 22 (2001) 189–200.
[28] N.G. Polikhronidi, I.M. Abdulagatov, R.G. Batyrova, Features of isochoric heat capacity measurements near the phase transition points, Fluid Phase Equilib. 201 (2002) 269–286.
[29] N.G. Polikhronidi, I.M. Abdulagatov, J.W. Magee, G.V. Stepanov, Isochoric heat capacity measurements for heavy water near the critical point, Int. J. Thermophys. 23 (2002) 745–770.
[30] N.G. Polikhronidi, I.M. Abdulagatov, J.W. Magee, G.V. Stepanov, Isochoric heat capacity measurements for an equimolar light and heavy water mixture in the near-critical and supercritical regions, Int. J. Thermophys. 24 (2003) 405–428.
[31] W. Wagner, A. Pruß, The IAPWS formulation 1995 for the thermodynamic properties of ordinary water substance for general and scientific use, J. Phys. Chem. Ref. Data 31 (2002) 387–535.
[32] N.B. Vargaftik, Handbook of Physical Properties of Liquids and Gases, second ed., Hemisphere, New York, 1983.
[33] I.K. Kamilov, G.V. Stepanov, I.M. Abdulagatov, A.R. Rasulov, E.I. Milikhina, Liquid–liquid–vapor, and liquid–vapor phase transitions in aqueous *n*-hexane mixtures from isochoric heat capacity measurements, J. Chem. Eng. Data 46 (2001) 1556–1567.
[34] V.M. Valyashko, I.M. Abdulagatov, J.H.M. Levelt-Sengers, Vapor–liquid–solid phase transitions in aqueous sodium sulfate and sodium carbonate from heat capacity measurements near the first critical endpoint: Part II. The phase boundaries, J. Chem. Eng. Data 45 (2000) 1139–1149.
[35] E.W. Lemmon, R. Span, Short fundamental equations of state for industrial fluids, (2003), in preparation.
[36] R. Span, W. Wagner, A new equation of state for carbon dioxide covering the fluid region from the triple-point temperature to 1100 K at pressures up to 800 MPa, J. Phys. Chem. Ref. Data 25 (1996) 1509–1596.
[37] J.C. Rainwater, Asymptotic expansions for constant-composition dew-bubble curves near the critical locus, Int. J. Thermophys. 10 (1989) 357–368.
[38] M.A. Anisimov, Critical Phenomena in Liquids and Liquid Crystals, Gordon and Breach, Philadelphia, 1991.
[39] M.A. Anisimov, E.E. Gorodezkii, V.D. Kulikov, J.V. Sengers, Crossover between vapor–liquid and consolute critical phenomena, Phys. Rev. E 51 (1995) 1199–1225.
[40] M.A. Anisimov, E.E. Gorodezkii, V.D. Kulikov, A.A. Povopdyrev, J.V. Sengers, A general isomorphism approach to thermodynamic and transport properties of binary fluid mixtures near the critical points, Physica A 220 (1995) 277–324.
[41] M.A. Anisimov, J.V. Sengers, in: J.V. Sengers, R.F. Kayser, C.J. Peters, H.J. White Jr. (Eds.), Equations of State for Fluids and Fluids Mixtures, Elsevier, Amsterdam, 2000, p. 381.
[42] M.E. Fisher, Renormalization of the critical exponents by hidden variables, Phys. Rev. B 176 (1968) 257–271.
[43] Kh.S. Abdulkadirova, A. Wyczalkowska, M.A. Anisimov, J.V. Sengers, Thermodynamic properties of mixtures of H_2O and D_2O in the critical region, J. Chem. Phys. 116 (2002) 4597–4610.
[44] P.C. Albright, T.J. Edwards, Z.Y. Chen, J.V. Sengers, A scaled fundamental equation for the thermodynamic properties of carbon dioxide in the critical region, J. Chem. Phys. 87 (1987) 1717–1725.
[45] J.V. Sengers, J.M.H. Levelt Sengers, Critical phenomena in classical fluids, in: C.A. Croxton (Ed.), Progress in Liquid Physics, Wiley, New York, 1978, p. 103.
[46] I.R. Krichevskii, Thermodynamics of critical phenomena in infinitely dilute binary solutions, Russ. J. Phys. Chem. 41 (1967) 1332–1338.
[47] J.M.H. Levelt Sengers, G. Morrison, G. Nielson, R.F. Chang, C.M. Everhart, Thermodynamic behavior of supercritical fluid mixtures, Int. J. Thermophys. 7 (1986) 231–243.
[48] M. Roth, Krichevskii parameter of heavy n-alkanes in carbon dioxide: comparison of the results from solubility measurements and from supercritical fluid chromatography, Fluid Phase Equilib. 212 (2003) 1–9.
[49] T. Furuya, A.S. Teja, Krichevskii parameters and solubility of heavy n-alkanes in supercritical carbon dioxide, Ind. Eng. Chem. Res. 39 (2000) 4828–4830.
[50] G.S. Gurdial, N.R. Foster, S.L.J. Yun, K.D. Tilly, Phase behavior of supercritical fluid-entrainer systems, in: Supercritical Fluid Engineering Sciences. Fundamentals and Applications. ACS Symposium Ser. 514, Washington, DC, 1993, pp. 34–45.
[51] N.G. Polikhronidi, R.G. Batyrova, I.M. Abdulagatov, J.W. Magee, G.V. Stepanov, (2003), in preparation.
[52] A.I. Abdulagatov, G.V. Stepanov, I.M. Abdulagatov, The crossover equation of state and micro-structural properties of the infinitely dilute solutions near the critical point of pure solvent, Russ. J. Struct. Chem. 42 (2001) 585–597.